

Cite this: *Chem. Sci.*, 2021, 12, 11038

All publication charges for this article have been paid for by the Royal Society of Chemistry

Received 8th June 2021  
Accepted 10th July 2021

DOI: 10.1039/d1sc03121j

rsc.li/chemical-science

# Directed Markovnikov hydroarylation and hydroalkenylation of alkenes under nickel catalysis†

Zi-Qi Li, Omar Apolinar, Ruohan Deng and Keary M. Engle \*

We report a full account of our research on nickel-catalyzed Markovnikov-selective hydroarylation and hydroalkenylation of non-conjugated alkenes, which has yielded a toolkit of methods that proceed under mild conditions with alkenyl sulfonamide, ketone, and amide substrates. Regioselectivity is controlled through catalyst coordination to the native Lewis basic functional groups contained within these substrates. To maximize product yield, reaction conditions were fine-tuned for each substrate class, reflecting the different coordination properties of the directing functionality. Detailed kinetic and computational studies shed light on the mechanism of this family of transformations, pointing to transmetalation as the turnover-limiting step.

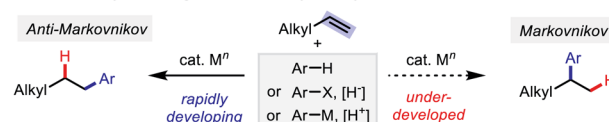
## Introduction

Catalytic alkene functionalization is an efficient and economical way to build up molecular complexity from readily accessible chemical feedstocks.<sup>1</sup> Transition-metal-catalyzed alkene hydroarylation/alkenylation reactions, in particular, represent a straightforward means of constructing C(sp<sup>3</sup>)-C(sp<sup>2</sup>) bonds. Various strategies have been developed to control regioselectivity using both conjugated and non-conjugated alkenes, with the latter introducing added complications from alkyl-metal chain-walking.<sup>2–7</sup> Anti-Markovnikov hydroarylation methods with non-conjugated alkenes have developed rapidly during the past several years.<sup>8–12</sup> In these systems selectivity control typically stems from the thermodynamic preference for formation of a primary alkylmetal intermediate. Markovnikov-selective hydroarylation reactions with non-conjugated alkenes, on the other hand, are comparatively rare, with research in this area progressing more slowly (Scheme 1A).<sup>13</sup> A notable advance was reported by Shenvi and co-workers 2016, who developed a dual-catalytic Co/Ni metal-hydride H-atom-transfer (MHAT) approach that was effective for the hydroarylation of terminal alkenes with aryl halides, where regioselectivity is controlled by the favorable formation of a secondary alkyl radical *via* MHAT.<sup>13c</sup>

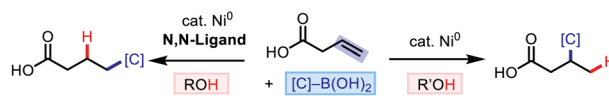
Pioneered by Zhou and co-workers, nickel(0)-catalyzed redox-neutral hydroarylation enables robust coupling of alkenes and arylboronic acids in alcohol solvents.<sup>2i–k</sup> Building on foundational work by Zhou using conjugated alkene substrates (*i.e.*,

styrenes and 1,3-dienes)<sup>2i</sup> and later contributions by Zhao using non-conjugated alkenyl carboxamides bearing a bidentate directing auxiliary,<sup>7c,d</sup> we recently developed a ligand-controlled regiodivergent hydrofunctionalization of simple non-conjugated alkenyl carboxylates. Addition of a carefully tailored Pyrox ligand allowed toggling of regioselectivity, bringing about either anti-Markovnikov or Markovnikov selectivity (Scheme 1B).<sup>14</sup> Contemporaneously, Wang and co-workers developed an electron-rich diimine ligand to promote nickel(II)-catalyzed anti-Markovnikov-selective hydroarylation of a range of different non-conjugated terminal alkenes with arylboronic acids.<sup>15</sup> Expanding the scope of Markovnikov-selective hydroarylation to other classes of non-conjugated alkene starting materials bearing native functional groups beyond carboxylic

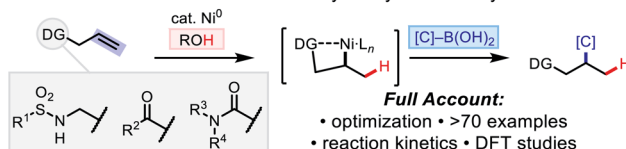
### A. Metal-Catalyzed Regioselective Hydroarylation Reactions



### B. Regiodivergent Hydrofunctionalization of Alkenyl Carboxylate (Ref. 14)



### C. This work: Directed Markovnikov Hydroarylation/alkenylation



Scheme 1 Background and synopsis of current work.

Department of Chemistry, The Scripps Research Institute, 10550 North Torrey Pines Road, La Jolla, California 92037, USA. E-mail: keary@scripps.edu

† Electronic supplementary information (ESI) available. See DOI: 10.1039/d1sc03121j

acids<sup>16</sup> would enhance the preparative utility of this approach. Moreover, understanding the underlying mechanism with greater clarity would support further improvements in scope, selectivity, and efficiency. To this end, in the present study, we report the nickel(0)-catalyzed hydroarylation and -alkenylation of alkenyl sulfonamides,<sup>16c</sup> ketones,<sup>16e</sup> and amides<sup>16d</sup> and investigate the reaction mechanism (Scheme 1C). Across all three substrate classes, high Markovnikov-selectivity arises from substrate directivity without the need for an ancillary ligand.

## Results and discussion

To initiate our investigation, we tested various model substrates under the reaction conditions previously optimized to bring about hydroarylation of alkenyl carboxylate substrates.<sup>14</sup> However, only moderate to low yields were observed (8–66% yield, Scheme 2, right column). Evaluation of different reaction conditions revealed that each of the individual substrate classes responded differently to changes in key reaction variables. Practically speaking, this observation prompted us to optimize reaction conditions that were tailored for each substrate class, as summarized in Scheme 2. A series of cross-compatibility experiments reveals the extent to which the fine-tuned reaction conditions are substrate-specific. Comparing the optimal conditions for each substrate illustrates common features and important differences that shed light on mechanistic features of this methodology (see below). In all cases the reactions proceed under relatively mild temperatures (rt – 40 °C), in contrast to analogous non-directed reactions that generally require elevated temperatures ( $\geq 80$  °C).<sup>24,15</sup> Additionally, alcohol solvent

was required in all of the protocols, reflecting solvent participation in the key hydronickelation process. Tuning of the steric bulk and  $pK_a$  for individual substrates presumably serves to control the rate of this step. The optimal inorganic base, both in identity and loading, also varied across substrate class. The base is critically involved in promoting and thus modulating the rate of organoboron transmetalation, but it can also play a deleterious role in mediating alkene isomerization with alkenyl amide and especially alkenyl ketone substrates bearing acidic  $\alpha$ -C–H bonds. This latter point required lower base equivalents (5 mol% LiOt-Bu) or weaker base (2 equiv.  $\text{Cs}_2\text{CO}_3$ ), respectively, be used for these two substrate families. It is worth mentioning that even though we screened a wide breadth of different ligands, there was no sign of ligand-based regiodivergence as was reported with alkenyl carboxylates (see ESI†).<sup>14</sup> The mechanistic origin of this point remains unclear, though one possible explanation is that the metal is already coordinatively saturated with ligands that cannot be readily displaced in the selectivity determining step (see below).

Having identified effective conditions for each family of substrates, we then proceeded to evaluate the scope of each of the three protocols. First, we examined the method for alkenyl sulfonamides,<sup>17</sup> where the best conditions were found to be KOH (2 equiv.) as base and *t*-AmylOH as solvent at room temperature (Table 1). Apart from a moderate yield obtained with electron-rich methoxy substitution at the *para*-position (2c), electronic variation of arylboronic acid does not affect the yield significantly, and products 2a–2j were prepared in good to excellent yield. When the reaction was performed on 0.6 mmol scale, 2f was obtained in 99% yield. A potentially coordinating

Reaction scheme:  $\text{DG}-(\text{CH}_2)_n + \text{Ar-B(OH)}_2 + \text{Ni(cod)}_2 (10 \text{ mol}\%) \xrightarrow{\text{[conditions as below]}} \text{DG}-(\text{CH}_2)_n-\text{Ar}$

Base: 2 equiv KOH, 2 equiv  $\text{Cs}_2\text{CO}_3$ , 5 mol% LiOt-Bu, 2 equiv KOt-Bu  
 Solvent: *t*-AmylOH, *s*-BuOH, *i*-PrOH, *n*-BuOH  
 Temperature: r.t., 40 °C, 40 °C  
 Time: 20 h

Substrate	2 equiv KOH, <i>t</i> -AmylOH, r.t.	2 equiv $\text{Cs}_2\text{CO}_3$ , <i>s</i> -BuOH, 40 °C	5 mol% LiOt-Bu, <i>i</i> -PrOH, 40 °C	2 equiv KOt-Bu, <i>n</i> -BuOH, 40 °C [Ref. 14]
TsHN-CH <sub>2</sub> -CH=CH <sub>2</sub>	99%	38%	9%	50%
PMP-CH <sub>2</sub> -CH=CH <sub>2</sub>	39%	99% <sup>b</sup> [62%] <sup>c</sup>	99% [ $<5\%$ ] <sup>c</sup>	66%
BnHN-CH <sub>2</sub> -CH=CH <sub>2</sub>	28%	15%	99%	8%
HOOC-CH <sub>2</sub> -CH=CH <sub>2</sub>	$<5\%$	38%	$<5\%$	99%

Legend: 0–40% (light blue), 40–80% (medium blue), 80–100% (dark blue)

**Scheme 2** Cross-compatibility of reaction conditions. <sup>a</sup>All percentages represent <sup>1</sup>H NMR yields of combined regioisomers with  $\text{CH}_2\text{Br}_2$  as internal standard. PMP = 4-methoxyphenyl. <sup>b</sup>Reaction time was 2 h instead of 20 h to prevent potential ester exchange with solvent. <sup>c</sup>Value in brackets represents the reaction outcome using *p*-TolB(OH)<sub>2</sub> as coupling partner.

**Table 1** Markovnikov-selective hydrofunctionalization of alkenyl sulfonamides<sup>a</sup>

Reaction scheme:  $\text{TsHN-CH}_2\text{-CH=CH}_2 + \text{[C]-B(OH)}_2 \xrightarrow{\text{Ni(cod)}_2 (10 \text{ mol}\%), \text{KOH (2.0 equiv)}, \text{t-AmylOH, r.t., 20 h}} \text{TsHN-CH}_2\text{-CH}_2\text{-CH(Ar)-CH}_3$

**• Aryl- and Alkenylboronic Acid Scope**

Product	R	Yield (%)
2a	R=H	95%
2b	R=Me	90%
2c	R=OMe	56%
2d	R=F	93%
2e	R=CF <sub>3</sub>	94%
2f	R=CO <sub>2</sub> Me	82% [99%] <sup>b</sup>
2g	R=NHBoc	81%
2h	R= <i>t</i> -Bu	88%
2i	R=Ph	82%
2j	R=Cl	90%
2k	R=Me	90%
2l	R=F	89%
2m	R=CF <sub>3</sub>	99%
2n	R=CN	43%
2o	R=Ph	94%
2p	R=Ph	65%
2q	R=OMe	88%
2r	R=CF <sub>3</sub>	99%
2s	R=Ph	88%

**• Sulfonamide PG**

Product	R	Yield (%)
2t	R=Me	99%
2u	R=MeO	97%
2v	R=CF <sub>3</sub>	90%

PG =  $\text{Ns}$ ,  $\text{Cs}$ ,  $\text{Boc}$   
 limitations ( $<5\%$  yield)

<sup>a</sup> Reaction conditions: reactions performed on 0.1 mmol scale. Percentages represent isolated yields. <sup>b</sup> Value in brackets represents the isolated yield of a reaction performed on 0.6 mmol scale. <sup>c</sup> Ns = 4-nitrobenzenesulfonyl. Cs = 4-cyanobenzenesulfonyl.

*meta*-CN substituent gave 43% yield (**2n**). Other substituents on the *meta*-position were well tolerated (**2k–2m**). Excellent yield of **2o** (94%) was obtained with 2-naphthylboronic acid. With boronic acids bearing more complex substitution patterns, such as a benzodioxazole or 3,5-disubstitution, the reaction proceeded smoothly, giving **2p–2r** in good yield. Extension to the analogous hydroalkenylation reaction was successful, with **2s** obtained in 88% yield. Other substituents on the sulfonamide group were next tested. With a methanesulfonyl protecting group, quantitative yield was obtained (**2t**). The electronic influence of the arylsulfonamide was next probed by introducing different groups at the *para*-position, with **2u** (–OMe) and **2v** (–CF<sub>3</sub>) both formed in excellent yield. In terms of limitations, more electron-withdrawing substituents (–CN and –NO<sub>2</sub>) proved deleterious, with no desired product observed in either case. The lack of product formation in these cases may be due to the oxidizing nature of the arenesulfonyl groups, which could interfere with the nickel(0) catalyst, or alternatively to the attenuated  $\sigma$ -donor strength of the nitrogen atom. The *N*-sulfonyl group proved to be crucial for reactivity, as replacement with the commonly used *tert*-butyl carbamate (*N*-Boc) protecting group yielded only unreacted starting material, potentially reflecting distinct coordination chemistry between sulfonamides and carbamates.<sup>16d</sup>

We then turned our attention to  $\beta,\gamma$ -unsaturated ketone substrates, where cesium carbonate (2 equiv.) and *s*-BuOH were identified as optimal base and solvent, respectively, at a reaction temperature of 40 °C (Table 2). We first evaluated *para*-substituted arylboronic acid coupling partners with different electronic properties and found that higher yield was obtained with boronic acids bearing an electron-withdrawing substituent (**4ac–4ad**). A representative example (**4ad**) was performed on 0.6 mmol scale, and 79% yield was obtained. Although the initial attempt towards **4aa** only offered 37% yield, a higher yield could be achieved by using a higher catalyst loading or boronic acid loading. Electronic or steric modifications at the *meta*-position do not have a significant effect on reaction efficiency, with **4ae–4aj** generated in good yields. Potentially reactive electrophilic substituents were well tolerated (**4ag** and **4ai**). When *ortho*-substituted arylboronic acids were employed, higher yield was observed with electron-deficient aryl groups (**4al** and **4am**), while moderate yield (36%) was obtained with *ortho*-tolylboronic acid (**4ak**). High-yielding hydroalkenylation was achieved with both aryl- and alkyl-substituted alkenylboronic acids (**4an–4aq**). To our delight, heteroaryl boronic acids were tolerated in this reaction, giving products **4ar–4at** in moderate to good yield. Subsequently, we examined the scope of alkenyl ketone substrates. Within the aryl allyl ketones series, we found that a variety of aryl substituents were accommodated, leading to moderate to good yields (**4ba–4bj**). Alkyl-substituted ketones were also tolerated, though in the case of a cyclohexyl group (**4bl**), a diminished yield of 38% was obtained. To our delight,  $\alpha$ -methyl substituted alkenyl ketones gave the corresponding product in 85% yield with 3 : 1 dr (**4bm**). When internal alkene was tested, **4bn** was obtained in 56% yield. To showcase the synthetic utility of this reaction, the natural

Table 2 Markovnikov-selective hydrofunctionalization of alkenyl ketones<sup>a</sup>

<b>• (Hetero)aryl- and Alkenylboronic Acid Scope</b>		
<b>4aa</b> , R=Me, 37% (80%) <sup>b</sup>	<b>4af</b> , R=F, 72%	<b>4ae</b> , R=Me, 60%
<b>4ab</b> , R=F, 47%	<b>4ag</b> , R=Cl, 74%	<b>4af</b> , R=F, 72%
<b>4ac</b> , R=CF <sub>3</sub> , 72%	<b>4ah</b> , R=CF <sub>3</sub> , 76%	<b>4ag</b> , R=Cl, 74%
<b>4ad</b> , R=CO <sub>2</sub> Me, 99% [79%] <sup>c</sup>	<b>4ai</b> , R=COMe, 75%	<b>4ah</b> , R=CF <sub>3</sub> , 76%
	<b>4aj</b> , R=OBn, 76%	<b>4ai</b> , R=COMe, 75%
<b>4ak</b> , R=Me, 36%	<b>4an</b> , R= <i>p</i> -Tol, 85%	<b>4aj</b> , R=OBn, 76%
<b>4al</b> , R=F, 86%	<b>4ao</b> , R=4-CF <sub>3</sub> C <sub>6</sub> H <sub>4</sub> , 91%	<b>4an</b> , R= <i>p</i> -Tol, 85%
<b>4am</b> , R=CF <sub>3</sub> , 80%	<b>4ap</b> , R= <i>t</i> -Bu, 71%	<b>4ao</b> , R=4-CF <sub>3</sub> C <sub>6</sub> H <sub>4</sub> , 91%
<b>4ar</b> , 66% <sup>d</sup>	<b>4aq</b> , R= <i>n</i> -Bu, 63%	<b>4ap</b> , R= <i>t</i> -Bu, 71%
<b>4as</b> , 32% <sup>d</sup>		<b>4aq</b> , R= <i>n</i> -Bu, 63%
<b>4at</b> , 69% <sup>d</sup>		
<b>• Alkene Scope</b>		
<b>4ba</b> , R= <i>p</i> - <i>t</i> -Bu, 78%	<b>4bf</b> , 85%	<b>4bb</b> , R= <i>p</i> -F, 67%
<b>4bb</b> , R= <i>p</i> -F, 67%	<b>4bg</b> , 68%	<b>4bc</b> , R= <i>m</i> -Me, 91%
<b>4bc</b> , R= <i>m</i> -Me, 91%	<b>4bj</b> , 67%	<b>4bd</b> , R= <i>o</i> -F, 58%
<b>4bd</b> , R= <i>o</i> -F, 58%	<b>4bk</b> , 75%	<b>4be</b> , R= <i>o</i> -Me, 57%
<b>4bh</b> , 67%		
<b>4bi</b> , 43%		
<b>4bl</b> , 38%		
<b>4bm</b> , 85%, 3 : 1 dr		
<b>4bn</b> , 56% <sup>d</sup> [from ( <i>E</i> )-alkene]		
<b>4bo</b> , 36% (3 steps) turmerone		

<sup>a</sup> Reaction conditions: reactions performed on 0.1 mmol scale. Percentages represent isolated yields. PMP = 4-methoxyphenyl, Ar<sup>1</sup> = (4-methoxycarbonyl)phenyl. <sup>b</sup> Initial attempt with 5 mol% catalyst loading led to 37% isolated yield. When 10 mol% catalyst loading was applied, 58% isolated yield was obtained. Yield in parentheses was obtained with 3.0 equiv. of *p*-TolB(OH)<sub>2</sub> and 5 mol% catalyst loading. <sup>c</sup> Reaction time was 2 h instead of 20 h to prevent potential ester exchange with solvent. Value in brackets represents the isolated yield of a reaction performed on 0.6 mmol scale. <sup>d</sup> Reaction performed with 10 mol% catalyst loading.

product (*rac*)-turmerone was synthesized in three steps from commercially available starting materials.<sup>18</sup>

Having tested sulfonamide and ketone directing groups, our focused then shifted to amide-based substrates.  $\beta,\gamma$ -Unsaturated amides were found to be prone to isomerization when stoichiometric base was used. Gratifyingly, when catalytic LiOt-Bu (5 mol%) in *i*-PrOH was employed, both hydroarylation and hydroalkenylation of alkenyl amides proceeded smoothly (Table 3). Generally speaking, compared the analogous ketone-containing substrates, alkenyl amides react with lower regioselectivity. With the exception of *para*-(trifluoromethyl)phenylboronic acid (**6a**), which delivered only 45% yield, alteration of the electronic properties of the *para*-substituent did not affect the yield or selectivity in a significant way (**6b–6e**). When performed on larger scale, **6e** was obtained in excellent yield with slightly lower regioselectivity. Electron-donating or

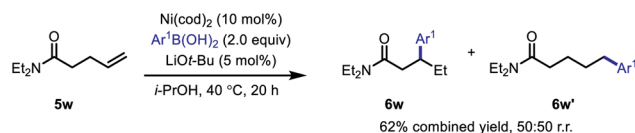


**Table 3** Markovnikov-selective hydrofunctionalization of alkenyl amides<sup>a</sup>

<b>• Aryl- and Alkenylboronic Acid Scope</b>	
	6a, R=CF <sub>3</sub> , 45%, 90:10 r.r.
	6b, R=Me, 77%, 93:7 r.r.
	6c, R=OMe, 85%, 94:6 r.r.
	6d, R=Ph, 67%, 90:10 r.r.
	6e, R=CO <sub>2</sub> Me, 81%, 91:9 r.r.
[97%, 87:13 r.r.] <sup>b</sup>	
<b>• Alkene Scope</b>	
	6f, R=OMe, 94%, 92:8 r.r.
	6g, R=CF <sub>3</sub> , 94%, 90:10 r.r.
	6h, R=F, 86%, 91:9 r.r.
	6i, R=Cl, 35%, 87:13 r.r.
	6j, R=PMP, 95%, >95:5 r.r.
	6k, R=t-Bu, 68%, >95:5 r.r.
	6l, R=n-Hex, 72%, >95:5 r.r.
	6m, 82%, 90:10 r.r.
	6n, 80%, 89:11 r.r.
	6o, 69%, 93:7 r.r.
	6p, 69%, 86:14 r.r.
	6q, 86%, 92:8 r.r.
	6r, 87%, 89:11 r.r.
	6s, 94%, 93:7 r.r.
	6t, 88%, 97:3 r.r.
	6u, 88%, 86:14 r.r.
	6v, 86%, 95:5 r.r.

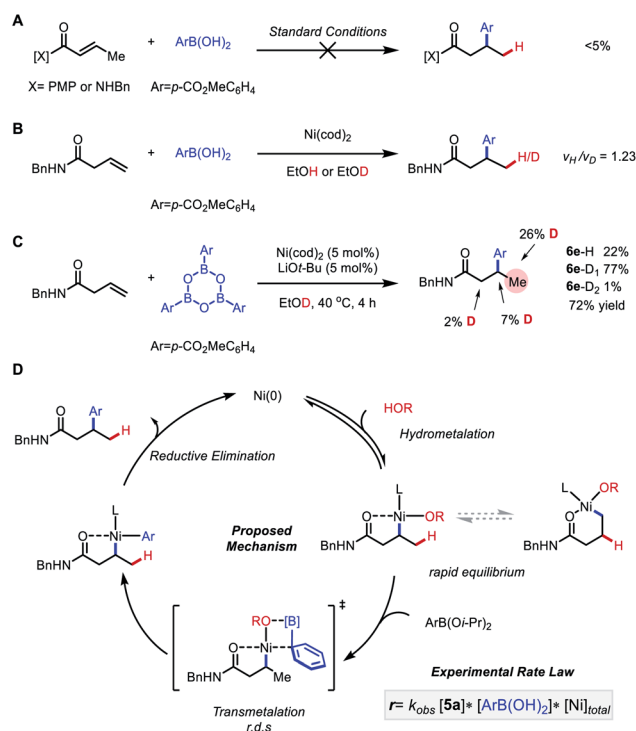
<sup>a</sup> Reactions performed on 0.1 mmol scale. Unless otherwise noted, percentages represent combined isolated yield of the two regioisomers, which were inseparable by silica gel chromatography. Regioisomeric ratio (r.r.) values represent Markovnikov/anti-Markovnikov product ratios, as determined *via* <sup>1</sup>H NMR analysis of isolated product mixtures. These values were generally consistent ( $\pm 5\%$ ) with those determined directly from the crude reaction mixture. Ar<sup>1</sup> = (4-methoxycarbonyl)phenyl. <sup>b</sup> Values in brackets represent the isolated yield and r.r. of a reaction performed on 0.6 mmol scale.

-withdrawing groups at the *meta*-position gave high yield and regioselectivity of approximately 90 : 10 (**6f–6h**), whereas a potentially reactive *meta*-chloro-substituent gave 35% yield (**6i**). When alkenylboronic acids were used, Markovnikov-selective hydroalkenylation took place with even higher regioselectivity (>95 : 5, **6j–6l**). Attenuated steric hindrance of the alkenylboron coupling partners compared to their aryl counterparts might account for the improved regioselectivity, since this could result in preferential stabilization of the selectivity-determining transmetalation transition state at a five-membered (and more hindered) secondary alkyl nickelacycle (leading to the Markovnikov-selective product) compared to at a six-membered (and less hindered) primary alkyl nickelacycle (leading to the anti-Markovnikov-selective product) (see below). Representative alkenyl amides were then tested to explore the scope and limitations of this method. Both secondary and tertiary amides were tolerated. *N*-(2,6-Dimethylphenyl)-substituted alkenyl amide gave 82% yield and 90 : 10 r.r. (**6m**). *N*-Alkyl-, *N,N*-dialkyl-, and *N*-alkyl-*N*-aryl-substituted amides gave moderate to good yield (**6n–6v**). Cyclic tertiary amides exhibited higher regioselectivity (**6t**, **6v**). Notably, when  $\gamma,\delta$ -unsaturated amide was tested, 62% combined yield was obtained of a 1 : 1 mixture of  $\beta$ - (**6w**) and  $\delta$ -arylated (**6w'**) isomers, resulting from carbonyl-directed migratory hydroarylation<sup>19</sup> and anti-Markovnikov hydroarylation, respectively (Scheme 3). This observation indicates that the favorable formation of a five-

**Scheme 3** Reactivity with a representative  $\gamma,\delta$ -unsaturated alkene substrate. Reaction performed on 0.1 mmol scale using standard conditions from Table 3. Ar<sup>1</sup> = (4-methoxycarbonyl)phenyl.

membered nickelacycle provides the driving force for selectivity and that alkylmetal chain walking (or metallacycle contraction) can take place when larger, less stable, metalacycles are formed upon initial hydronickelation. Formation of **6w'** may result from a competitive non-directed pathway.

A detailed mechanistic study was performed to shed more light on the mechanism of the transformation (Scheme 4). First, to exclude a tandem isomerization/1,4-addition mechanism, the  $\alpha,\beta$ -unsaturated amide and ketone that would be formed upon isomerization were tested under the optimal conditions. Only trace amounts (<5%) of the corresponding products were observed, which rules out this alternative pathway. Next, hydroarylation of *N*-benzyl  $\beta,\gamma$ -unsaturated amide was chosen as a model reaction for detailed kinetic investigation. In a kinetic isotope effect (KIE) experiment, we found  $v_H/v_D = 1.23$ , suggesting that hydrometallation might not be involved in the

**Scheme 4** Mechanistic experiments. Percentages represent <sup>1</sup>H NMR yields with CH<sub>2</sub>Br<sub>2</sub> as internal standard. (A) Control experiment with  $\alpha,\beta$ -unsaturated ketone/amide as substrate. (B) KIE study of Markovnikov selective hydroarylation of alkenyl amide. (C) Deuterium incorporation study with ethanol-*d*<sub>1</sub> as solvent. (D) Proposed catalytic cycle and experimental rate law, as determined by initial rate measurement and proposed mechanism.



turnover-limiting step. In comparison,  $\nu_{\text{H}}/\nu_{\text{D}} = 2.7$  was found in our previous study of Markovnikov-selective hydroarylation of alkenyl carboxylates.<sup>14</sup> This distinction indicates that a different mechanism or a different turnover-limiting step is operative in this system.<sup>20</sup> Deuterium labeling experiments using EtOD as solvent and boroxine as aryl source were conducted, showing deuterium incorporation mainly on the  $\gamma$ -position with scrambling on the  $\alpha$  and  $\beta$ -positions to some extent. Both the deuterium scrambling and the presence of double deuterated product suggests that a reversible hydrometalation step is operative before the selectivity-determining step. To disambiguate between transmetalation and reductive elimination being turnover-limiting step, the experimental rate law was determined using the method of initial rates (see ESI† for detail). We found  $\text{rate} = k_{\text{obs}}[\mathbf{5a}][\text{ArB}(\text{OH})_2][\text{Ni}]_{\text{total}}$ . This result is consistent with transmetalation being the turnover-limiting step. Altogether, the data are consistent with the following mechanism. First, hydrometalation proceeds through a reversible mechanism. Though a discrete Ni–H intermediate cannot be ruled out at this stage,<sup>24,7c,d</sup> a series of related studies have recently pointed to concerted hydronickelation being lower in energy.<sup>3c,14,21</sup> Either scenario would result in a common 5-membered alkyl nickelacycle, which rapidly equilibrates between with the corresponding 6-membered species, corresponding to Markovnikov and anti-Markovnikov selectivity, respectively. Next, turnover-limiting and selectivity-determining transmetalation takes place, followed by reductive elimination to furnish the desired product.

To gain a better understanding of the origin of regioselectivity, we next considered the turnover-limiting transmetalation step and the subsequent reductive elimination step computationally (Scheme 5).<sup>22</sup> Despite the formation of

a sterically and electronically disfavored secondary alkyl nickel species, the Markovnikov-selective pathway is still favored compared to the anti-Markovnikov-selective pathway by 1.0 kcal mol<sup>−1</sup> in the transmetalation step. The same trend was observed when comparing the corresponding intermediates (**7\_a** and **7\_m**). A structural analysis of these intermediates revealed a shorter bond length between the directing group and the nickel center in **7\_m** (1.92 Å) compared to **7\_a** (1.95 Å). This result indicates the formation of a stable five-membered metallocycle with the directing group is the key contributing factor for overcoming the thermodynamic preference of the formation of a primary alkyl nickel species. When alkenyl ketone was used as substrate, a larger energy barrier ( $\Delta\Delta G_{\text{sol}} = 2.4$  kcal mol<sup>−1</sup>) was observed, which explains the higher regioselectivity obtained experimentally (see ESI† for detail). Subsequent C(sp<sup>3</sup>)–C(sp<sup>2</sup>) reductive elimination steps were found to have comparatively low barriers of 17.3 and 16.7 kcal mol<sup>−1</sup> for **TS2\_m** and **TS2\_a**, respectively, with ethylene as model ligand for the different olefins that could coordinate under the reaction conditions (*i.e.*, COD, substrate, or alkene-containing product). This model stems from previous work demonstrating that  $\pi$ -accepting ligands promote the otherwise high-energy C–C reductive elimination events.<sup>16</sup>

## Conclusions

In summary, we established a series of reliable protocols for Markovnikov-selective hydroarylation/alkenylation of alkenes bearing a sulfonamide, ketone or amide as a directing group. With the support from a detailed mechanistic study, we found transmetalation is likely the turnover-limiting and selectivity-determining step. A computational study revealed that the directing-group-controlled formation of a five-membered alkyl nickel species is the origin of high Markovnikov selectivity.

## Data availability

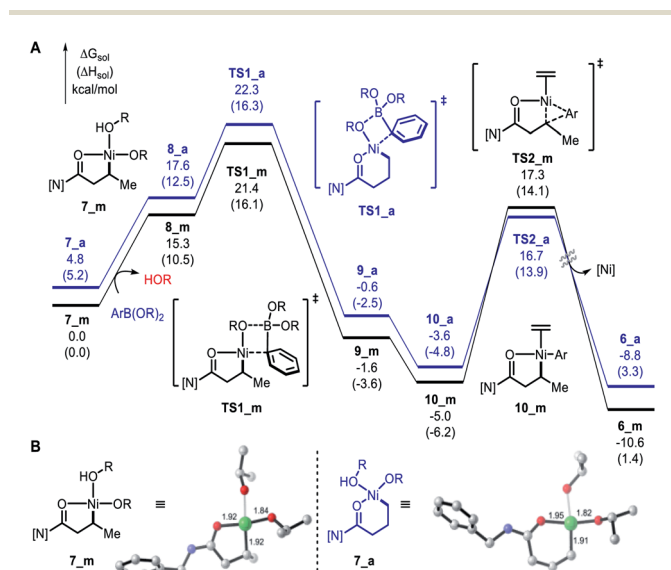
All experimental procedures and data related to this study can be found in the ESI. Original NMR data for the products (in MNova format) are included in a master ZIP file.

## Author contributions

Z.-Q. L. and K. M. E. conceived the project. Z.-Q. L. optimized the reaction conditions and evaluated scope. Z.-Q. L., O. A., and R. D. synthesized the starting materials. Z.-Q. L. performed computational and experimental mechanistic studies. Z.-Q. L. and K. M. E. wrote the manuscript with input from the other authors.

## Conflicts of interest

There are no conflicts to declare.



**Scheme 5** (A) Computed energy profile of the hydroarylation of **5a**. Calculations were performed at the B3LPY/SDD-6-311+G(d,p), SMD(2-propanol)//B3LYP/SDD-6-31G(d) level of theory. (B) Structural analysis of intermediate **7\_a** and **7\_m**. Bond distances are in angstroms.



## Acknowledgements

This work was financially supported by the National Science Foundation (CHE-1800280). We acknowledge the NSF for Graduate Research Fellowships (DGE-1842471 to O. A.). We thank Tanner C. Jenkins for careful proofreading and Prof. Peng Liu (University of Pittsburgh) for helpful discussion regarding the DFT studies.

## Notes and references

- For representative reviews, see: (a) Y. Yamamoto and U. Radhakrishnan, *Chem. Soc. Rev.*, 1999, **28**, 199–207; (b) R. I. McDonald, G. Liu and S. S. Stahl, *Chem. Rev.*, 2011, **111**, 2981–3019; (c) P. Gandeepan and C. H. Cheng, *Acc. Chem. Res.*, 2015, **48**, 1194–1206; (d) E. A. Standley, S. Z. Tasker, K. L. Jensen and T. F. Jamison, *Acc. Chem. Res.*, 2015, **48**, 1503–1514; (e) E. McNeill and T. Ritter, *Acc. Chem. Res.*, 2015, **48**, 2330–2343; (f) Y. C. Luo, C. Xu and X. Zhang, *Chin. J. Chem.*, 2020, **38**, 1371–1394; (g) Z. Liu, Y. Gao, T. Zeng and K. M. Engle, *Isr. J. Chem.*, 2020, **60**, 219–229; (h) J. Diccianni, Q. Lin and T. Diao, *Acc. Chem. Res.*, 2020, **53**, 906–919; (i) J. Derosa, O. Apolinar, T. Kang, V. T. Tran and K. M. Engle, *Chem. Sci.*, 2020, **11**, 4287–4296.
- For representative examples of hydroarylation of styrenes, see: (a) S. Torii, H. Tanaka and K. Morisaki, *Chem. Lett.*, 1985, **14**, 1353–1354; (b) G. Bhalla, J. Oxgaard, W. A. Goddard and R. A. Periana, *Organometallics*, 2005, **24**, 3229–3232; (c) Y. Iwai, K. M. Gligorich and M. S. Sigman, *Angew. Chem., Int. Ed.*, 2008, **47**, 3219–3222; (d) Y.-P. Xiao, X.-Y. Liu and C.-M. Che, *J. Organomet. Chem.*, 2009, **694**, 494–501; (e) G. E. M. Crisenza, N. G. McCreanor and J. F. Bower, *J. Am. Chem. Soc.*, 2014, **136**, 10258–10261; (f) S. D. Friis, M. T. Pirnot and S. L. Buchwald, *J. Am. Chem. Soc.*, 2016, **138**, 8372–8375; (g) K. Semba, K. Ariyama, H. Zheng, R. Kameyama, S. Sakaki and Y. Nakao, *Angew. Chem., Int. Ed.*, 2016, **55**, 6275–6279; (h) L. Jin, J. Qian, N. Sun, B. Hu, Z. Shen and X. Hu, *Chem. Commun.*, 2018, **54**, 5752–5755; (i) L.-J. Xiao, L. Cheng, W.-M. Feng, M.-L. Li, J.-H. Xie and Q.-L. Zhou, *Angew. Chem., Int. Ed.*, 2018, **57**, 461–464; (j) Y.-G. Chen, B. Shuai, X.-T. Xu, Y.-Q. Li, Q.-L. Yang, H. Qiu, K. Zhang, P. Fang and T.-S. Mei, *J. Am. Chem. Soc.*, 2019, **141**, 3395–3399; (k) X.-Y. Lv, C. Fan, L.-J. Xiao, J.-H. Xie and Q.-L. Zhou, *CCS Chem.*, 2019, **1**, 328–334; (l) X.-W. Yang, D.-H. Li, A.-X. Song and F.-S. Liu, *J. Org. Chem.*, 2020, **85**, 11750–11765; (m) L. J. Oxtoby, Z.-Q. Li, V. T. Tran, T. G. Erbay, R. Deng, P. Liu and K. M. Engle, *Angew. Chem., Int. Ed.*, 2020, **59**, 8885–8890.
- For representative examples of hydroarylation of 1,3-dienes, see: (a) L. Liao and M. S. Sigman, *J. Am. Chem. Soc.*, 2010, **132**, 10209–10211; (b) J. S. Marcum, C. C. Roberts, R. S. Manan, T. N. Cervarich and S. J. Meek, *J. Am. Chem. Soc.*, 2017, **139**, 15580–15583; (c) J. S. Marcum, T. R. Taylor and S. J. Meek, *Angew. Chem., Int. Ed.*, 2020, **59**, 14070–14075; (d) T. Hamaguchi, Y. Takahashi, H. Tsuji and M. Kawatsura, *Org. Lett.*, 2020, **22**, 1124–1129.
- For a review and representative examples of hydroarylation of  $\alpha,\beta$ -unsaturated carbonyl compounds, see: (a) T. Hayashi and K. Yamasaki, *Chem. Rev.*, 2003, **103**, 2829–2844; (b) A. M. Vasquez, J. A. Gurak Jr, C. L. Joe, E. C. Cherney and K. M. Engle, *J. Am. Chem. Soc.*, 2020, **142**, 10477–10484; (c) S. Cacchi and A. Arcadi, *J. Org. Chem.*, 1983, **48**, 4236–4240.
- For representative examples of hydroarylation of heteroatom-substituted alkenes, see: (a) S. Bera and X. Hu, *Angew. Chem., Int. Ed.*, 2019, **58**, 13854–13859; (b) S. Cuesta-Galisteo, J. Schörghöner, X. Wei, E. Merino and C. Nevado, *Angew. Chem., Int. Ed.*, 2021, **60**, 1605–1609; (c) Y. He, H. Song, J. Chen and S. Zhu, *Nat. Commun.*, 2021, **12**, 638.
- For representative examples of hydroarylation reactions involving chain-walking, see: (a) Y. He, Y. Cai and S. Zhu, *J. Am. Chem. Soc.*, 2017, **139**, 1061–1064; (b) Y. He, C. Liu, L. Yu and S. Zhu, *Angew. Chem., Int. Ed.*, 2020, **59**, 9186–9191; (c) Y. Zhang, B. Han and S. Zhu, *Angew. Chem., Int. Ed.*, 2019, **58**, 13860–13864.
- For recent examples involving bidentate directing auxiliaries, see: (a) C. Wang, G. Xiao, T. Guo, Y. Ding, X. Wu and T.-P. Loh, *J. Am. Chem. Soc.*, 2018, **140**, 9332–9336; (b) R. Matsuura, T. C. Jenkins, D. E. Hill, K. S. Yang, G. M. Gallego, S. Yang, M. He, F. Wang, R. P. Marsters, I. McAlpine and K. M. Engle, *Chem. Sci.*, 2018, **9**, 8363–8368; (c) H. Lv, L.-J. Xiao, D. Zhao and Q.-L. Zhou, *Chem. Sci.*, 2018, **9**, 6839–6843; (d) H. Lv, H. Kang, B. Zhou, X. Xue, K. M. Engle and D. Zhao, *Nat. Commun.*, 2019, **10**, 5025.
- For reviews of anti-Markovnikov-selective hydroarylation of non-conjugated alkenes with Ar–H coupling partners, see: (a) F. Kakiuchi and S. Murai, *Acc. Chem. Res.*, 2002, **35**, 826–834; (b) L. Yang and H. Huang, *Chem. Rev.*, 2015, **115**, 3468–3517; (c) Z. Dong, Z. Ren, S. J. Thompson, Y. Xu and G. Dong, *Chem. Rev.*, 2017, **117**, 9333–9403. For recent report involving Ni(0) catalysis, see: (d) N. I. Saper, A. Ohgi, D. W. Small, K. Semba, Y. Nakao and J. F. Hartwig, *Nat. Chem.*, 2020, **12**, 276–283.
- For recent examples of anti-Markovnikov-selective hydroarylation and alkylation of non-conjugated alkenes involving a silane as the hydride source, see: (a) X. Lu, B. Xiao, Z. Zhang, T. Gong, W. Su, J. Yi, Y. Fu and L. Liu, *Nat. Commun.*, 2016, **7**, 11129; (b) J. Nguyen, A. Chong and G. Lalic, *Chem. Sci.*, 2019, **10**, 3231–3236; (c) Z. Wang, H. Yin and G. C. Fu, *Nature*, 2018, **563**, 379–383.
- For examples of reductive Heck hydroarylation of non-conjugated alkenes, see ref. 2h and 7a, and the following: (a) J. A. Gurak Jr and K. M. Engle, *ACS Catal.*, 2018, **8**, 8987–8992. For a review, see: (b) L. J. Oxtoby, J. A. Gurak Jr, S. R. Wisniewski, M. D. Eastgate and K. M. Engle, *Trends Chem.*, 2019, **1**, 572–587.
- S. D. Friis, M. T. Pirnot, L. N. Dupuis and S. L. Buchwald, *Angew. Chem., Int. Ed.*, 2017, **56**, 7242–7246.
- T. Liu, Y. Yang and C. Wang, *Angew. Chem., Int. Ed.*, 2020, **59**, 14256–14260.



- 13 For recent dual catalytic examples involving hydrogen-atom-transfer, see: (a) S. A. Green, J. L. M. Matos, A. Yagi and R. A. Shenvi, *J. Am. Chem. Soc.*, 2016, **138**, 12779–12782; (b) S. A. Green, S. Vasquez-Céspedes and R. A. Shenvi, *J. Am. Chem. Soc.*, 2018, **140**, 11317–11324; (c) S. L. Shevick, C. Obradors and R. A. Shenvi, *J. Am. Chem. Soc.*, 2018, **140**, 12056–12068.
- 14 Z.-Q. Li, Y. Fu, R. Deng, V. T. Tran, Y. Gao, P. Liu and K. M. Engle, *Angew. Chem., Int. Ed.*, 2020, **59**, 23306–23312.
- 15 D.-M. Wang, W. Feng, Y. Wu, T. Liu and P. Wang, *Angew. Chem., Int. Ed.*, 2020, **59**, 20399–20404.
- 16 (a) J. Derosa, R. Kleinmans, V. T. Tran, M. K. Karunananda, S. R. Wisniewski, M. D. Eastgate and K. M. Engle, *J. Am. Chem. Soc.*, 2018, **140**, 17878–17883; (b) V. T. Tran, Z.-Q. Li, T. J. Gallagher, J. Derosa, P. Liu and K. M. Engle, *Angew. Chem., Int. Ed.*, 2020, **59**, 7029–7034; (c) J. Derosa, T. Kang, V. T. Tran, S. R. Wisniewski, M. K. Karunananda, T. C. Jenkins, K. L. Xu and K. M. Engle, *Angew. Chem., Int. Ed.*, 2020, **59**, 1201–1205; (d) O. Apolinar, V. T. Tran, N. Kim, M. A. Schmidt, J. Derosa and K. M. Engle, *ACS Catal.*, 2020, **10**, 14234–14239; (e) R. Kleinmans, O. Apolinar, J. Derosa, M. K. Karunananda, Z.-Q. Li, V. T. Tran, S. R. Wisniewski and K. M. Engle, *Org. Lett.*, 2021, **23**, 5311–5316.
- 17 M. Miura, T. Tsuda, T. Satoh, S. Pivsa-Art and M. Nomura, *J. Org. Chem.*, 1998, **63**, 5211–5215.
- 18 P. P. Mahulikar and R. B. Mane, *J. Chem. Res.*, 2006, **2006**, 15–18.
- 19 Substrate-directed, migratory alkene functionalization *via* hydronickelelation has been previously documented. For oxidative Heck arylation, see ref. 7c. For hydroalkylation, see: (a) X. Chen, W. Rao, T. Yang and M. J. Koh, *Nat. Commun.*, 2020, **11**, 5857. For related nickelacycle contraction processes in 1,3-dicarbonyl functionalization, see: (b) W. Li, J. K. Boon and Y. Zhao, *Chem. Sci.*, 2018, **9**, 600–607; (c) P. Basnet, R. K. Dhungana, S. Thapa, B. Shrestha, S. KC, J. M. Sears and R. Giri, *J. Am. Chem. Soc.*, 2018, **140**, 7782–7786.
- 20 In addition, it might also explain our inability to identify effective ligands to promote anti-Markovnikov-selective hydrofunctionalization with these substrates, despite extensive screening (see ESI† for detail).
- 21 (a) F. Wang and Q. Meng, *J. Org. Chem.*, 2020, **85**, 13264–13271; (b) Q. Cheng and Y. Dang, *Org. Lett.*, 2020, **22**, 8998–9003.
- 22 Because the present reaction system does not employ traditional nitrogen- or phosphine-based ancillary ligands, it is difficult to unambiguously establish the preferred coordination environment in the hydronickelelation step, which as discussed above also has an unclear mechanism. Due to these uncertainties we were not confident that DFT studies of this step would be conclusive. Additionally, given that hydronickelelation was empirically determined not to be involved in the turnover-limiting step, we decided to focus the DFT studies on the transmetalation and subsequent reductive elimination steps.

